J Mater Sci (2006) 41:8339–8346
DOI 10.1007/s10853-006-1029-0

Al–Ti powder produced through mechanical alloying for different times

F. G. Cuevas · J. Cintas · J. M. Montes · J. M. Gallardo

Received: 4 August 2004 / Accepted: 14 October 2005 / Published online: 28 October 2006

Abstract A powder mixture of aluminum, 10 wt% titanium, and 1.5 wt% of a wax acting as process control agent (PCA), has been attrition-milled for 2–20 h. Titanium powder had been previously ground to a lower particle size to make it similar to the as-received aluminum particle size. The overall aim of this work was to achieve a metastable titanium solution in the aluminum matrix. Changes with milling time of particle size and shape, microstructure, hardness and other powder characteristics have been studied. Given the used experimental-conditions, a process time of 10 h has been selected for the mechanical alloying (MA) of Al–10Ti powder, attaining a compromise between uniform microstructure development and a not so long processing time. At this milling time aluminum dissolves about 9 wt% Ti, increasing its Vickers microhardness (202 VH_{20}) more than 10 times with reference to the starting Al powder (20 VH_{20}). Milled particle size is smaller than the starting one (17 vs. 44 μm). Increasing milling for longer times, up to 20 h, does not produce important changes in powders structure.

Introduction

Mechanical alloying (MA) is a well-known powder producing process developed around mid-60 s by Benjamin [1]. In recent years, MA has outpassed the scope of a method for producing composite metal powders with a fine microstructure. The process has been employed to obtain alloys with extended solubility, amorphous materials, nanocrystalline structures and to synthesize inorganic compounds [2–9].

In the Al rich part of the Al–Ti system, metaestable Al–Ti solid solutions may be produced by this technique. Milling Al–Ti pre-alloyed powder, Al and Al_3Ti powders, or Al and Ti elemental powders, produces intermetallic Al-Ti dispersoids on annealing or even during milling. These dispersoids help to refine grain size and to dispersion strengthen the MA Al. In addition, Al_3Ti has a low density [10].

The properties of specific materials obtained by MA are very sensitive to experimental conditions (milling type, energy input, type and amount of PCA, atmosphere, etc.) [2–7]. In this research, Al and Al–10Ti powder have been prepared by attrition milling in the presence of a wax. After selecting the experimental conditions, the evolution of microstructure and properties of the powders with milling time has been studied. The main purpose was to achieve a homogeneous powder amenable to powder metallurgy (PM) processing.

Materials and experimental procedure

A commercial-grade atomized powder from Eckart-Werke (Fürth, Germany) has been used as raw Al powder. Its purity is better than 99.7%, the main impurity being 0.15 wt% Fe. Particle size is smaller than 125 μm, with a mean particle size of 44 μm. Titanium powder has been supplied by Deeside

F. G. Cuevas (✉) · J. Cintas · J. M. Montes · J. M. Gallardo
Department of Mechanical and Materials Engineering, Escuela Superior de Ingenieros, Universidad de Sevilla, Camino de los Descubrimientos s/n, E-41092 Sevilla, Spain
e-mail: fgcuevas@us.es

Titanium Ltd, Deeside, UK. Certified titanium content is <99.4%. As-received Ti particle size has been considered too big (mean particle size of 145 μm) to produce a fine and well-dispersed Al–Ti phase. Titanium powder has then been slightly ground in high vacuum atmosphere, for 10 min, in the presence of 0.5 wt% of a wax (Hoechst Micropowder C wax, $H_{35}C_{17}CONHC_2H_4NHCOC_{17}H_{35}$, smaller than 40 μm) acting as PCA. A fraction of milled Ti powder, smaller than 62 μm, has been screened to be employed as Ti starting powder, with a final mean particle size of 56 μm.

Mixtures of Al and 10 wt% Ti starting powders, along with 1.5% of the wax, have been milled under confined air or vacuum atmosphere (better than 5 Pa). Milling times from 2 to 20 h have been selected to follow the powder properties evolution. Milling machine is a Szegvari attritor [11] (Union Process), a vertical ball mill where the grinding balls are agitated by a rotating impeller (Fig. 1). Other milling conditions, shown in Table 1, have been chosen according to the experimental results from preliminary studies [12]. Pure Al powder has been milled in similar conditions for comparison.

Powder particles size distribution has been measured according to ASTM B214-86 Standard Method. Laser diffraction technique has also been used for particle size distribution measurement.

Metallographic observations on polished specimens have been performed on a scanning electron microscope (SEM), operated at 10 kV. A back scattered electrons (BSE) detector has been used for phase identification, while powder morphology is studied with the secondary electrons (SE) signal. Quantification of undissolved Ti in the Al powder matrix has been carried out. These pure Ti areas in the Al–Ti agglomerated powder particles may be clearly distinguished as a separate phase in BSE-SEM micrographs. On the other hand, the presence of free Ti particles, randomly distributed in the metallographic specimen, is frequent in the initial steps. Therefore, the quantification of free Ti particles is very time-consuming, and was not performed.

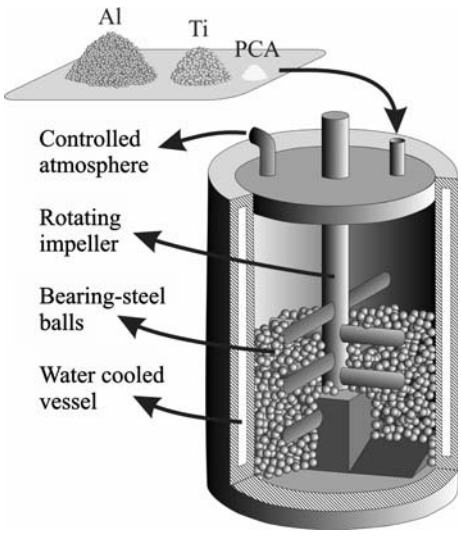

Fig. 1 Attritor-type ball mill

Table 1 Milling conditions for Al and Al-10Ti powders

Operating parameters	
Miller model	Szegvari attritor
Vessel volume	1400 cm^3
Balls: powder ratio	3600 g: 72 g (50:1)
Balls diameter	4.65 mm
PCA	Wax
PCA content	1.5%
Rotor speed	500 rpm
Cooling	H_2O flow (18 °C)
Milling time	2–20 h

X-ray measurements have been performed with a powder diffractometer, using the Cu K_α (λ = 1.54183 Å) radiation. Step-scanning has been carried out from 20 to 120° (2θ), with a counting time of 5 s every 0.02°. The Rietveld method [13] has been used in the quantitative analysis of the samples.

Vickers microhardness measurements, according to ASTM E 384-99e1 Standard Method, have been carried out under a load of 0.02 kg (VH_{20}). Factors considered in these measurements were: type of resin, resin curing time, powder particle size, initial distance indenter-specimen and approach speed of the indenter, applied load and time of application. Considering the aforementioned Standard and the influence of the factors considered, the small fraction of powder particles bigger than 75 μm, 6 times the size of the indentation, were inserted in a polyester resin, cured for 8 days, and polished and dried following PM processing methods. The indenter was placed at about 0.75 mm, and an approach speed of 0.12 mm/s (the main factor affecting the measurements) was used. The load, with a maximum deviation of 0.15 g, was applied for 10 s in order to attain the equilibrium in the system.

PM properties such as powders apparent density (the mass of a powder divided by its apparent volume, ASTM B 212-99), tap density (the apparent powder density obtained under stated conditions of tapping, ASTM B 527-93(2000)e1) and flowability (the ability of a powder to flow, ASTM B 213-97) have been determined using well-established common methods.

Results and discussion

Pre-milled Ti powder

After milling, Ti powder has a planar morphology. This morphology, typical of the first stages of MA processes, is due to the short milling time employed. However, milling for 10 min is enough to reduce Ti powder particle size. Powders morphology, after screening the fraction smaller than 62 μm, is shown in Fig. 2. As received Al powder is also included in this figure for comparison.

Al-10 wt% Ti after vacuum-milling up to 10 h

Particle size. Particle size distribution of Al–10Ti, milled under vacuum atmosphere (Al–10Ti/V) for 2, 4, 6, 8 and 10 h, can be seen in Fig. 3. It shows an alternating behavior of coarsening and refining tendencies as milling time increases. Nevertheless, the final (10 h) particle size distribution, obtained by sieve analysis, is similar to the initial one. A clear tendency to grow exists during the first 2 h. Then, as the powder hardens, a certain steady-state size distribution is achieved, which, after 6 h, evolves towards particle fracture, decreasing the particle size. Similar milling experiences with pure aluminum show a higher coarsening tendency than in milling the Al–10Ti mixture. Hardening effect of the dissolved Ti, along with the lower ductility of Ti, probably prevents powders welding and coarsening to the extent observed in the case of pure Al. Particle size distribution for both powders—pure Al and Al–10Ti-, after being milled for 10 h under vacuum atmosphere, is plotted in Fig. 4.

Particle morphology and structure

Figures 5 and 6 display the changes in powder particle morphology and structure, respectively, occurring during attrition milling of Al–Ti powder up to 10 h. Four stages can be distinguished in the MA process, namely, flake particles formation, flake particles welding (multilayered Al–Ti agglomerated flakes), rounding of particles (convoluted structure) and particle equiaxing and homogenizing.

During the first 2 h of milling, the original particles initially flatten into flakes (stage 1). In addition, some flaky-particles weld together, giving way to a multilayered structure (stage 2). At this stage, individual particles of Al and Ti, without mixing, can also be distinguished (Fig. 6, top). Plate-shaped particles (Fig. 5, top) are thicker than the initial powder particles.

After the process is under way for 4 h, the multilayered elongated particles are transformed to a relatively equiaxed shape (stage 3). Multilayered flakes fold and/or break and reweld without any preferred orientation, causing a convoluted structure. This process goes on for 6 h (Fig. 5 and 6, middle). Titanium areas (clear strings in the figure) are progressively finer.

For milling times of 8 and 10 h, the powder is rather equiaxed and relatively rounded-shaped (Fig. 5, bottom). The internal layered-structure disappears (stage 4), being replaced by a homogeneous dispersion/alloying of Ti (Fig. 6, bottom). Once the final stage of milling is reached for 10 h, nearly all Ti is dissolved in the Al matrix.

The changes in particle morphology and structure reported in this investigation are roughly in agreement with the findings of Benjamin and Volin [14], during the MA of a mixture of Fe and Cr powders in a high-energy shaker mill.

Results of quantitative metallography on SEM micrographs are shown in Fig. 7. Two curves are included: the percentage area of Ti patches, and the number of Ti patches per unit area, both measured on the agglomerated powder particles. As mentioned above, free non-agglomerated Ti particles are not taken into account. The area percentage of Ti is continuously growing till 4 h milling time, due to the incorporation of new free Ti particles to the Al matrix.

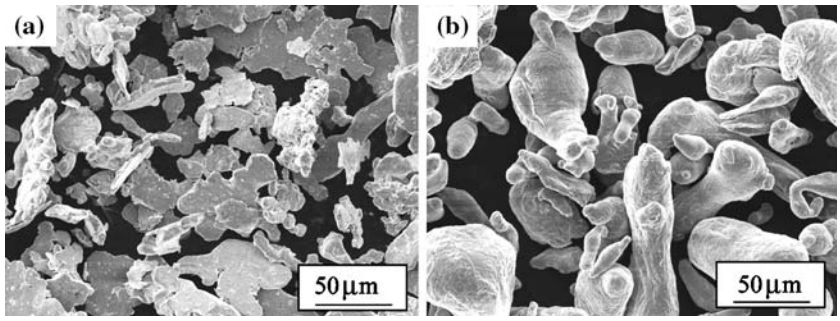

Fig. 2 SE-SEM micrographs showing starting powders morphology: (**a**) 10 min vacuum-milled Ti, smaller than 62 μm, (**b**) as received Al powder

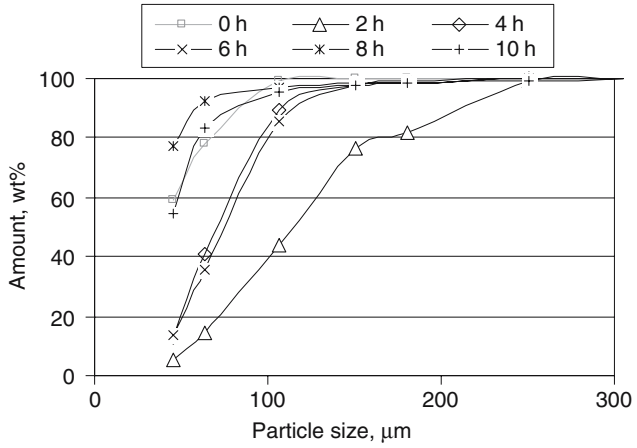

Fig. 3 Cumulative weight percentage of Al–10Ti/V particles finer than a given size as milling time increases

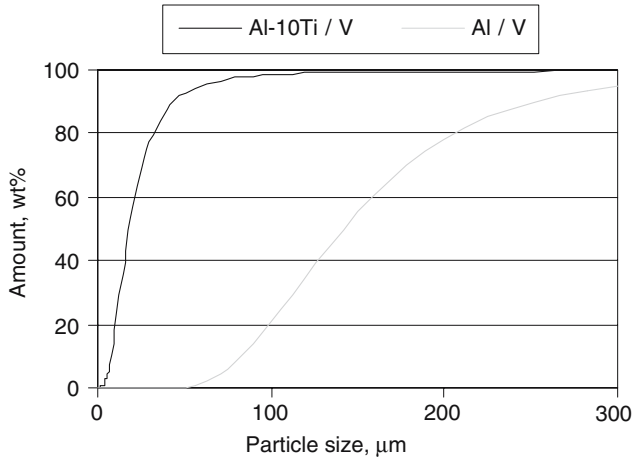

Fig. 4 Cumulative weight percentage of particles finer than a given size, for 10 h milling

On the other hand, the number of titanium ''chips'' (patches), per unit area of the Al matrix, is continually growing till 6 h milling time. This could be explained by the formation of multilayered structures and the shredding of incorporated-to-the-matrix Ti particles. Afterwards, the dissolution process accounts for the observed decrease of undissolved Ti. After 10 h, these Ti chips have a mean size of 270 nm.

Increasing milling time will very slowly complete the dissolution of the added Ti.

X-ray measurements

XRD patterns (Fig. 8) show a progressive disappearance of Ti peaks with milling time, along with Al-peak broadening and displacement. These phenomena may be related to the increasing degree of alloying of Ti atoms in the Al matrix. Neither intermetallics nor

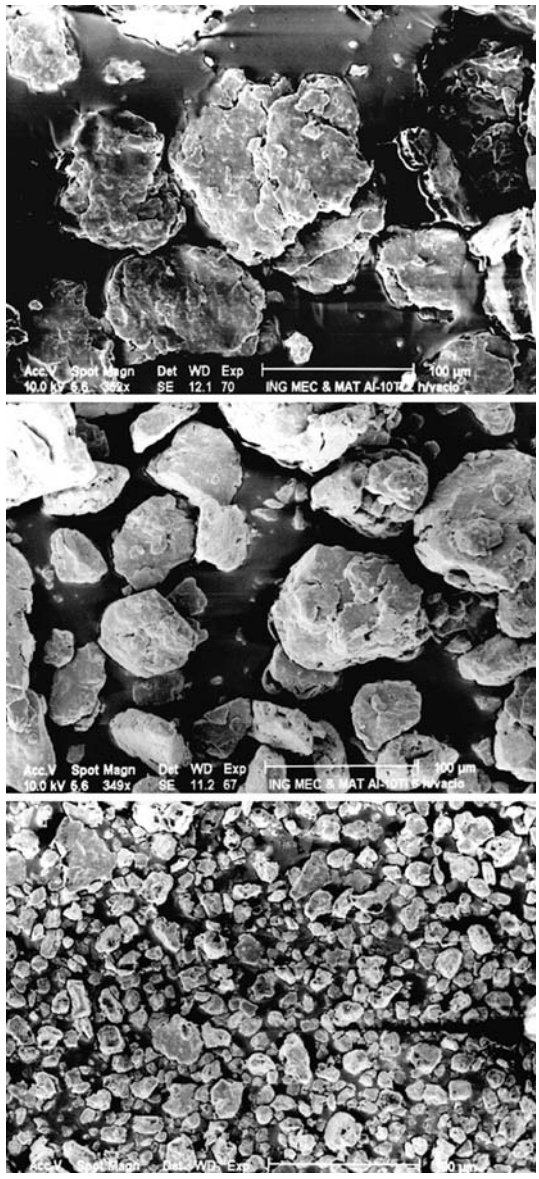

Fig. 5 SE-SEM micrographs showing the morphologies of Al–10Ti/V powder after milling for various times. From top to bottom: 2, 6 and10 h

other compounds are observed at any milling stage. Table 2 includes some data drawn from quantitative measurements based on the diffraction patterns (Rietveld method). Numerical values for 10 h have to be taken with caution, due to experimental difficulties. Results from quantitative analysis of SEM micrographs are also included in the table, where area percentages of Ti embedded in the Al powder are expressed as weight percentage.

Increasing milling time produces a progressive disappearance of Ti, as separate crystals. After 10 h milling, nearly 90% of the initially added Ti is incorporated to the Al. This value is in good agreement

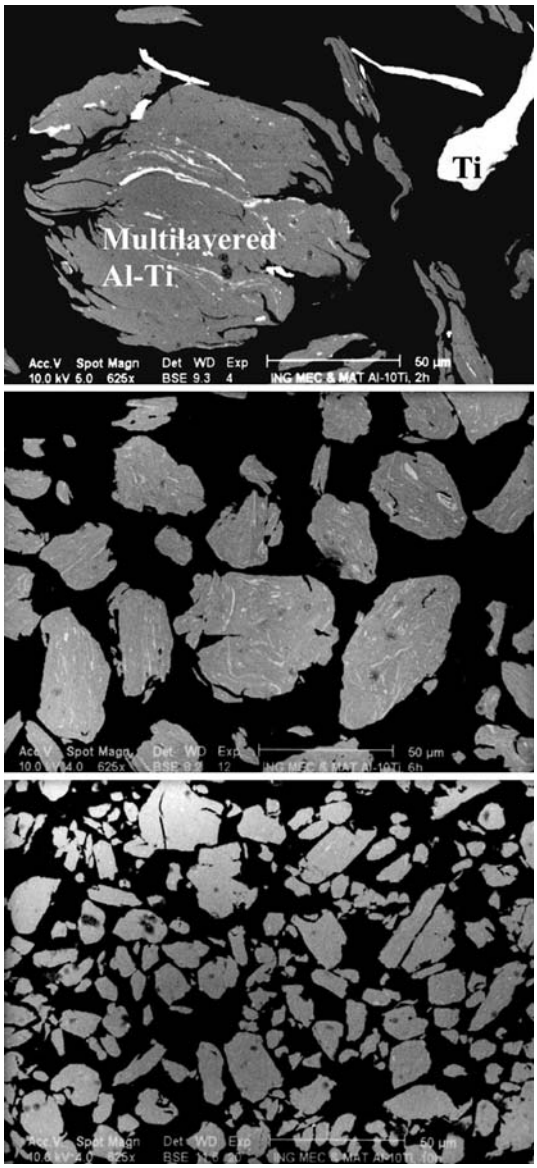

Fig. 6 BSE-SEM microstructures (transverse cross section) of Al–10Ti/V powder after milling for various times. From top to bottom: 2, 6 and 10 h

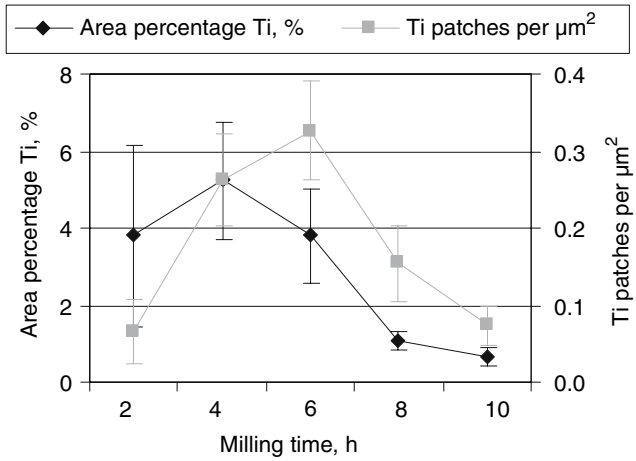

Fig. 7 Undissolved Ti versus milling time (SEM quantitative metallography) for Al–10Ti/V

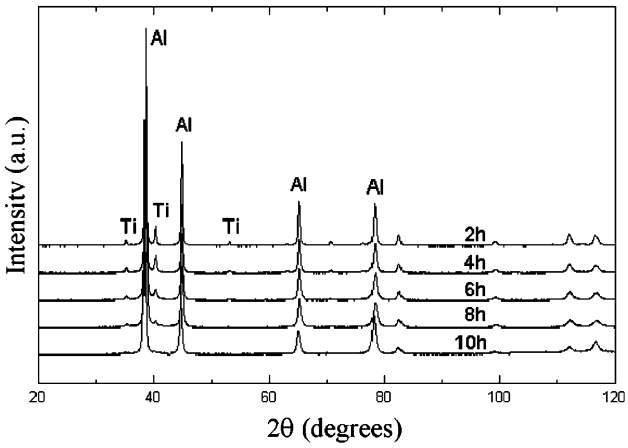

Fig. 8 Al–10Ti/V XRD patterns for different milling times

with quantitative metallography measurements. Only 10% of the added Ti can be distinguished in SEM micrographs (linear resolution for the magnification used is 100 nm). It may be concluded from these structural observations that the powder is becoming mechanically alloyed.

At the same time, shifting of aluminium peaks is related to a reduction of the lattice parameter, due to Ti dissolution in Al [15]. Milling also produces a crystallite size decrease, shown in Al peaks broadening. Al crystallite size after milling for 10 h is 20 nm, as measured on (111) peaks by the Rietveld́s method.

A special analysis is worth to be carried out on the lattice parameter evolution as a function of Ti content in the Al matrix. Very few data can be found in the literature for MA Al–Ti, and the discrepancy between them is quite big. So, linear decreases in the Al lattice parameter on increasing the dissolved Ti have been reported both at rates of 0.0054 [10] and 0.0009 Å [15] per 1 wt% Ti increase. As shown in Fig. 9, data obtained in this research is in agreement with the second mentioned source. However, all these values are obtained from the fitting analysis of XRD patterns

Table 2 Undissolved Ti (XRD and BSE-SEM measurements) and Al crystal parameter (XRD) as a function of milling time

Milled Al-10Ti/V	2 h	4 h	6 h	8 h	10 h
Undissolved Ti, as measured by XRD, wt%	8.2	8.8	6.6	2.7	1.6
Ti patches in Al particles (BSE-SEM), wt%	6.2	8.5	6.2	1.8	1.1
Al crystal parameter, Å	4.0498	4.0486	4.0478	4.0450	–

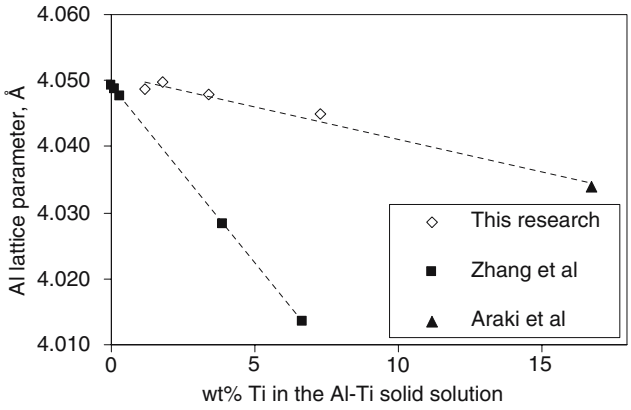

Fig. 9 Al lattice parameter versus Ti content in an Al–Ti solid solution

diffraction peaks, and more new data would be of interest to determine the actual evolution of the lattice parameter.

Microhardness

Powder microhardness varies with milling time due to changes in internal structure, as shown in Fig. 10. Milling produces a rapid, almost linear, increase in hardness over that of the starting powder. After 10 h milling, the microhardness (202 VH_{20}) is 10 times higher than at the beginning of processing (20 VH_{20} for Al powder). The high hardness of MA Al-10Ti is probably due to (a) crystallite size refinement and (b) alloying hardening brought about by Ti in metastable solution [5]. The full cold worked structure is most likely not retained, since high-energy grinding of Al may promote dynamic recovery. This could give rise to repeated subgrain formation and a final refined structure.

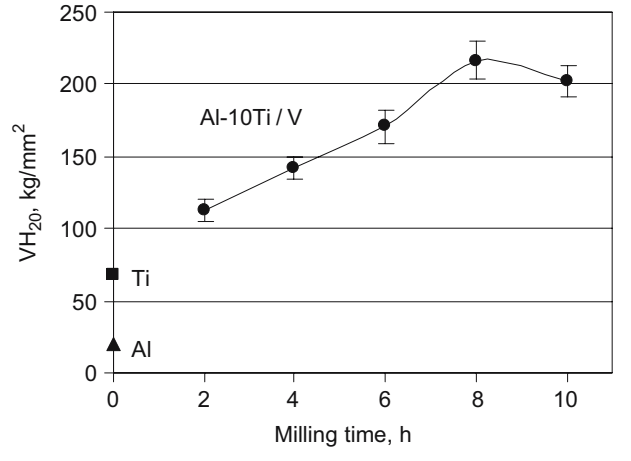

Fig. 10 Microhardness of Al, Ti and Al–Ti powders versus milling time

Other properties of the as-milled powders

Apparent and tap densities show the lowest values for 2 h milling time (Fig. 11), when relatively big and flaky particles exist. Round particles, not very fine in size, as for 4–6 h, present higher densities. The 10 h MA Al–10Ti powder, of the smallest size, has an intermediate relative apparent density of 1.05 g/cm^3, similar to the starting mixture.

Flowability can be explained in similar terms. Flaky and/or fine powders do not flow freely. On the other hand, powder milled during 4 and 6 h show free flowing behavior.

Air-millings longer than 10 h

As mentioned before, during the last 2 h (from 8 to 10 h) of milling, dissolution rate is very slow, what suggests that milling for longer times is little profitable.

Some milling runs up to 20 h are carried out in air. An air atmosphere is chosen for these long milling experiences as no difference is observed between air and vacuum atmospheres for Al–10Ti powder milled for 10 h [16]. Besides, air atmosphere does not require the use of any additional equipment. The presence of Ti is the reason to observe no difference between Al–10Ti powders milled in air and vacuum. For both atmospheres, particle size decreases up to values around 20 μm, because of Ti dissolution in the Al matrix, which hardens the powder and favors the fracture processes during milling. This hardening due to solid solution makes the atmosphere effect to be unappreciable. On the other hand, similar pure-Al millings show a particle size increase up to values of 65 and 140 μm for air and vacuum atmospheres. In this case, the hardening effect exerted by reaction with the PCA is relatively small, and particle sticking process

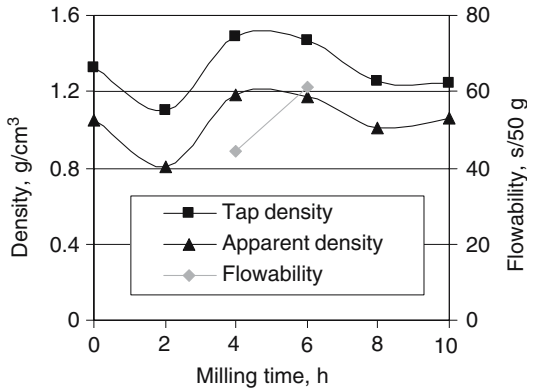

Fig. 11 Densities (apparent and tap) and flowability of as milled Al–10Ti/V powder

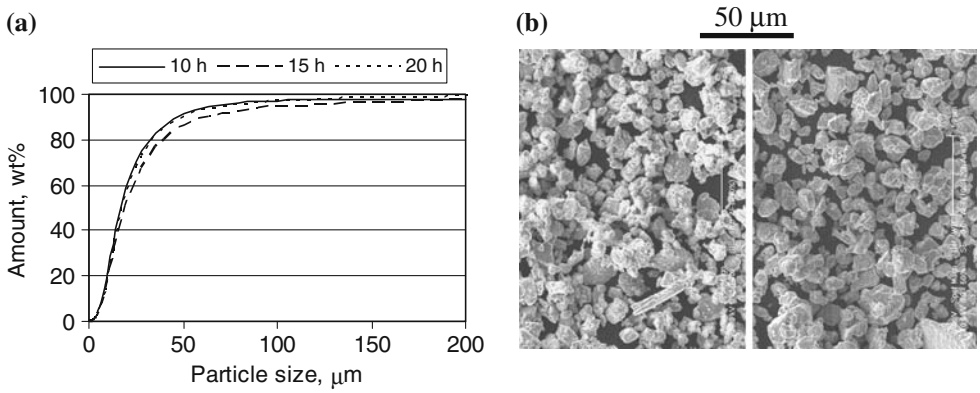

Fig. 12 (**a**) Cumulative wt% of Al–Ti particles finer than a given size. (**b**) SE-SEM micrographs showing powder morphology for Al–10Ti/A milled for 10 (left) and 20 (right) h

overpass fracture rate during milling. The lowest particle size obtained for air atmosphere is probably due to the formation of a thick alumina layer on the new Al powder surfaces exposed to the milling atmosphere, making more difficult the particles welding processes. This effect of air on new surfaces, changing their reactivity, has already been probed [17]. Another factor to be considered is the expectable lower PCA efficiency under vacuum atmosphere; a vacuum better than 5 Pa should easy the organic compound decomposition and, therefore, particle welding processes would be increased.

Fig. 12 shows that increasing milling time from 10 h to the maximum tested milling time (20 h) does not produce any significant particle morphology nor size changes. Round particles with mean particle sizes of 17, 20 and 18 μm are obtained after 10, 15 and 20 h milling, respectively.

In conclusion, particle size stabilization during MA occurs after 10 h milling for this Al-Ti system.

The evolution of the mean particle size with milling time during the whole milling process shows an initial increase and posterior decrease, reaching a final constant size. This behavior is also common for different milling systems [18, 19]. A shifted Gaussian curve is proposed in this paper to describe this evolution of the mean particle size, S, as a function of the milling time, t.

$$S = (S_M - S_\infty) \cdot \exp(-(t - t_M)^2/a^2) + S_\infty \quad (1)$$

where a is the fitting parameter, S_M the maximum size attained in the milling process (for a time t_M), S_∞ the final constant size, S_0 the initial mean particle size, and

$$t_M = a \cdot \sqrt{\ln((S_M - S_\infty)/(S_0 - S_\infty))}.$$

Figure 13 shows the evolution of the mean particle size during the milling process up to 20 h, together with the curve resulting from Eq. (1). The better correlation coefficient results to be $R^2 = 0.93$.

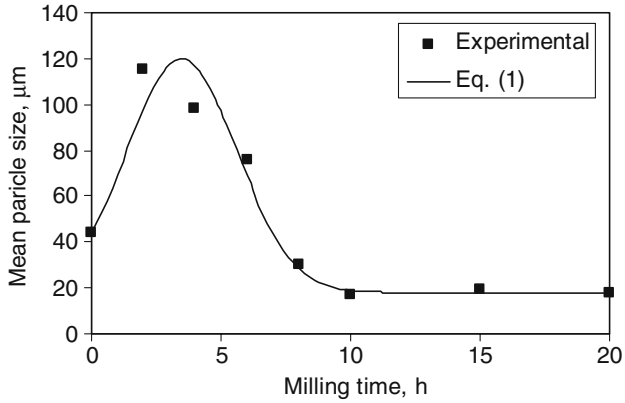

Fig. 13 Mean particle size of Al–10Ti powder (experimental data and fitting Eq. (1)) as a function of milling time (the fitting parameters are a = 3.0, S_M = 118, S_∞ = 18 and S_0 = 44.4)

Qualitative analysis of XRD patterns carried out on Al–10Ti/A milled for 10, 15 and 20 h, show that Ti peaks intensity decreases further for higher milling times, approaching a higher Ti dissolution in the Al matrix. It is worth noting that, although longer milling processes slightly change the internal powder structure, external powder shape and size remain unaffected.

Conclusions

The evolution of particle size, microstructure and other PM properties of Al–10Ti powder, milled in an attritor for 2–20 h, has been studied.

Particle size distribution varies with milling time, initially in the coarsening direction and, after 6 h, increasing particles fracture and refining. The starting irregular equiaxed particles change their morphology and structure through the stages of flattening, welding of parallel flakes, multilayered-flake folding, and

formation of relatively equiaxed particles with a homogeneous structure.

After 10 h milling, aluminum dissolves about 9 wt% Ti, obtaining a powder up to 10 times harder than the starting Al powder. All this titanium is in a metastable solution.

Increasing milling time for more than 10 h does not produce external structural changes in the powders. Internal structure slowly evolves to a higher dissolution of Ti.

In view of these results—for the equipment and processing conditions employed—a milling time of 10 h seems to be an optimum for the MA of the Al–10Ti powder. A compromise between uniform microstructure development and a not so long processing time is attained.

Acknowledgements This work was supported by the C.I.C. Y.T., Madrid, under research project DPI2005-03711.

References

1. Benjamin JS (1970) Met Trans 1(10):2943
2. Benjamin JS, Bomford MJ (1977) Met Trans 8A(8):1302
3. Jangg G (1975) Aluminium 51(10):641 (in German)
4. Gilman PS (1979) Ph.D. Thesis, Stanford University, USA
5. Singer RF, Oliver WC, Nix WD (1980) Met Trans 11A(11):1895
6. Bloch EA (1961) Met Rev 6:193
7. Froes FH, Suryanarayana C (1994) Metal Powder Rep 49(1):14
8. Moon KI, Park HS, Lee KS (2002) Mater Sci Eng A 323:293
9. Ma E, Atzmon M, Pinkerton FE (1993) J Appl Phys 74(2):955
10. Zhang F, Lu L, Lai MO (2000) J Alloys Comp 297(1–2):211
11. Szegvari A, Patent No. 2,764,359 (Sept. 25, 1956)
12. Rodríguez JA, (1992) Ph. D. Thesis, University of Seville, Spain
13. Young RA, (ed.) (2000) The Rietveld method (International Union of Crystallography), Oxford University Press, Oxford, UK
14. Benjamin JS, Volin TE (1974) Met Trans 5(8):1929
15. Araki H, Saji S, Okabe T, Minamino Y, Yamane T, Miyamoto Y (1995) Mater Trans JIM 36(3):465
16. Cuevas FG, (2004) Ph.D. Thesis, University of Seville, Spain
17. Ma E, Thompson CV, Clevenger LA (1991) J Appl Phys 69(4):2211
18. Ryu HJ, Hong SH, Baek WH (1997) J Mater Process Techol 63:292
19. Suryanarayana C (2001) Prog Mater Sci 46:1